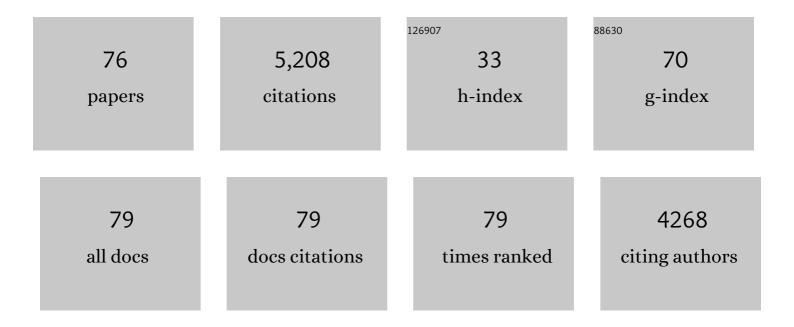
Florence Tama

List of Publications by Year in descending order

Source: https://exaly.com/author-pdf/8149028/publications.pdf Version: 2024-02-01



#	Article	IF	CITATIONS
1	Conformational change of proteins arising from normal mode calculations. Protein Engineering, Design and Selection, 2001, 14, 1-6.	2.1	796
2	Building-block approach for determining low-frequency normal modes of macromolecules. Proteins: Structure, Function and Bioinformatics, 2000, 41, 1-7.	2.6	421
3	Dynamic reorganization of the functionally active ribosome explored by normal mode analysis and cryo-electron microscopy. Proceedings of the National Academy of Sciences of the United States of America, 2003, 100, 9319-9323.	7.1	332
4	SYMMETRY, FORM, AND SHAPE: Guiding Principles for Robustness in Macromolecular Machines. Annual Review of Biophysics and Biomolecular Structure, 2006, 35, 115-133.	18.3	251
5	Structure of the E. coli protein-conducting channel bound to a translating ribosome. Nature, 2005, 438, 318-324.	27.8	243
6	Normal mode based flexible fitting of high-resolution structure into low-resolution experimental data from cryo-EM. Journal of Structural Biology, 2004, 147, 315-326.	2.8	230
7	Flexible Multi-scale Fitting of Atomic Structures into Low-resolution Electron Density Maps with Elastic Network Normal Mode Analysis. Journal of Molecular Biology, 2004, 337, 985-999.	4.2	217
8	Exploring Global Distortions of Biological Macromolecules and Assemblies from Low-resolution Structural Information and Elastic Network Theory. Journal of Molecular Biology, 2002, 321, 297-305.	4.2	193
9	The Mechanism and Pathway of pH Induced Swelling in Cowpea Chlorotic Mottle Virus. Journal of Molecular Biology, 2002, 318, 733-747.	4.2	190
10	Diversity and Identity of Mechanical Properties of Icosahedral Viral Capsids Studied with Elastic Network Normal Mode Analysis. Journal of Molecular Biology, 2005, 345, 299-314.	4.2	177
11	Mega-Dalton Biomolecular Motion Captured from Electron Microscopy Reconstructions. Journal of Molecular Biology, 2003, 326, 485-492.	4.2	113
12	Removal of Divalent Cations Induces Structural Transitions in Red Clover Necrotic Mosaic Virus , Revealing a Potential Mechanism for RNA Release. Journal of Virology, 2006, 80, 10395-10406.	3.4	106
13	Three-dimensional structure of the anthrax toxin pore inserted into lipid nanodiscs and lipid vesicles. Proceedings of the National Academy of Sciences of the United States of America, 2010, 107, 3453-3457.	7.1	102
14	Flexible Fitting of High-Resolution X-Ray Structures into Cryoelectron Microscopy Maps Using Biased Molecular Dynamics Simulations. Biophysical Journal, 2008, 95, 5692-5705.	0.5	101
15	Cell-based screen identifies a new potent and highly selective CK2 inhibitor for modulation of circadian rhythms and cancer cell growth. Science Advances, 2019, 5, eaau9060.	10.3	93
16	Iterative Elastic 3D-to-2D Alignment Method Using Normal Modes for Studying Structural Dynamics of Large Macromolecular Complexes. Structure, 2014, 22, 496-506.	3.3	90
17	Excited states of ribosome translocation revealed through integrative molecular modeling. Proceedings of the National Academy of Sciences of the United States of America, 2011, 108, 18943-18948.	7.1	89
18	The 13à Structure of a Chaperonin GroEL–Protein Substrate Complex by Cryo-electron Microscopy. Journal of Molecular Biology, 2005, 348, 219-230.	4.2	65

#	Article	IF	CITATIONS
19	Normal-Mode Flexible Fitting of High-Resolution Structure of Biological Molecules toward One-Dimensional Low-Resolution Data. Biophysical Journal, 2008, 94, 1589-1599.	0.5	62
20	Macromolecular structures probed by combining single-shot free-electron laser diffraction with synchrotron coherent X-ray imaging. Nature Communications, 2014, 5, 3798.	12.8	61
21	Isoform-selective regulation of mammalian cryptochromes. Nature Chemical Biology, 2020, 16, 676-685.	8.0	61
22	Electrostatic properties of cowpea chlorotic mottle virus and cucumber mosaic virus capsids. Biopolymers, 2006, 82, 106-120.	2.4	59
23	Molecular Model of a Soluble Guanylyl Cyclase Fragment Determined by Small-Angle X-ray Scattering and Chemical Cross-Linking. Biochemistry, 2013, 52, 1568-1582.	2.5	56
24	Bipartite anchoring of SCREAM enforces stomatal initiation by coupling MAP kinases to SPEECHLESS. Nature Plants, 2019, 5, 742-754.	9.3	55
25	Role of Computational Methods in Going beyond X-ray Crystallography to Explore Protein Structure and Dynamics. International Journal of Molecular Sciences, 2018, 19, 3401.	4.1	52
26	Dynamics at the serine loop underlie differential affinity of cryptochromes for CLOCK:BMAL1 to control circadian timing. ELife, 2020, 9, .	6.0	50
27	Normal Mode Analysis With Simplified Models To Investigate The Global Dynamics Of Biological Systems. Protein and Peptide Letters, 2003, 10, 119-132.	0.9	49
28	The Requirement for Mechanical Coupling Between Head and S2 Domains in Smooth Muscle Myosin ATPase Regulation and its Implications for Dimeric Motor Function. Journal of Molecular Biology, 2005, 345, 837-854.	4.2	47
29	Biased coarse-grained molecular dynamics simulation approach for flexible fitting of X-ray structure into cryo electron microscopy maps. Journal of Structural Biology, 2010, 169, 95-105.	2.8	47
30	Flexible fitting to cryo‣M density map using ensemble molecular dynamics simulations. Journal of Computational Chemistry, 2017, 38, 1447-1461.	3.3	46
31	Ribosome motions modulate electrostatic properties. Biopolymers, 2004, 74, 423-431.	2.4	44
32	Twelve Transmembrane Helices Form the Functional Core of Mammalian MATE1 (Multidrug and Toxin) Tj ETQqO	0	Overlock 10
33	Consensus among flexible fitting approaches improves the interpretation of cryo-EM data. Journal of Structural Biology, 2012, 177, 561-570.	2.8	38
34	Controlling the Circadian Clock with High Temporal Resolution through Photodosing. Journal of the American Chemical Society, 2019, 141, 15784-15791.	13.7	37
35	Reversible modulation of circadian time with chronophotopharmacology. Nature Communications, 2021, 12, 3164.	12.8	35

36Structures of human pannexin-1 in nanodiscs reveal gating mediated by dynamic movement of the N
terminus and phospholipids. Science Signaling, 2022, 15, eabg6941.3.634

#	Article	lF	CITATIONS
37	Replica Exchange Molecular Dynamics Simulations Provide Insight into Substrate Recognition by Small Heat Shock Proteins. Biophysical Journal, 2014, 106, 2644-2655.	0.5	32
38	Photopharmacological Manipulation of Mammalian CRY1 for Regulation of the Circadian Clock. Journal of the American Chemical Society, 2021, 143, 2078-2087.	13.7	31
39	Thermodynamic properties of water molecules in the presence of cosolute depend on DNA structure: a study using grid inhomogeneous solvation theory. Nucleic Acids Research, 2015, 43, gkv1133.	14.5	29
40	Phosphorylated Smooth Muscle Heavy Meromyosin Shows an Open Conformation Linked to Activation. Journal of Molecular Biology, 2012, 415, 274-287.	4.2	25
41	Integrative/Hybrid Modeling Approaches for Studying Biomolecules. Journal of Molecular Biology, 2020, 432, 2846-2860.	4.2	25
42	Allosteric Regulation of DNA Cleavage and Sequence-Specificity through Run-On Oligomerization. Structure, 2013, 21, 1848-1858.	3.3	23
43	Model of the toxic complex of anthrax: Responsive conformational changes in both the lethal factor and the protective antigen heptamer. Protein Science, 2006, 15, 2190-2200.	7.6	22
44	Steered Molecular Dynamics Simulations of a Type IV Pilus Probe Initial Stages of a Force-Induced Conformational Transition. PLoS Computational Biology, 2013, 9, e1003032.	3.2	22
45	Reconstruction of low-resolution molecular structures from simulated atomic force microscopy images. Biochimica Et Biophysica Acta - General Subjects, 2020, 1864, 129420.	2.4	21
46	Simulations of substrate transport in the multidrug transporter EmrD. Proteins: Structure, Function and Bioinformatics, 2012, 80, 1620-1632.	2.6	20
47	Consensus among multiple approaches as a reliability measure for flexible fitting into cryo-EM data. Journal of Structural Biology, 2013, 182, 67-77.	2.8	20
48	Topology representing neural networks reconcile biomolecular shape, structure, and dynamics. Neurocomputing, 2004, 56, 365-379.	5.9	19
49	Hybrid Electron Microscopy Normal Mode Analysis graphical interface and protocol. Journal of Structural Biology, 2014, 188, 134-141.	2.8	18
50	Hybrid approach for structural modeling of biological systems from X-ray free electron laser diffraction patterns. Journal of Structural Biology, 2016, 194, 325-336.	2.8	18
51	Structure modeling from small angle X-ray scattering data with elastic network normal mode analysis. Journal of Structural Biology, 2011, 173, 451-460.	2.8	16
52	Single-particle XFEL 3D reconstruction of ribosome-size particles based on Fourier slice matching: requirements to reach subnanometer resolution. Journal of Synchrotron Radiation, 2018, 25, 1010-1021.	2.4	16
53	Acceleration of cryo-EM Flexible Fitting for Large Biomolecular Systems by Efficient Space Partitioning. Structure, 2019, 27, 161-174.e3.	3.3	16
54	Molecular dynamics simulation shows large volume fluctuations of proteins. European Biophysics Journal, 2000, 29, 472-480.	2.2	15

#	Article	IF	CITATIONS
55	3DEM Loupe: analysis of macromolecular dynamics using structures from electron microscopy. Nucleic Acids Research, 2013, 41, W363-W367.	14.5	14
56	Three-dimensional reconstruction for coherent diffraction patterns obtained by XFEL. Journal of Synchrotron Radiation, 2017, 24, 727-737.	2.4	13
57	Structural differences in the FAD-binding pockets and lid loops of mammalian CRY1 and CRY2 for isoform-selective regulation. Proceedings of the National Academy of Sciences of the United States of America, 2021, 118, .	7.1	13
58	Local thermodynamics of the water molecules around single- and double-stranded DNA studied by grid inhomogeneous solvation theory. Chemical Physics Letters, 2016, 660, 250-255.	2.6	12
59	Network visualization of conformational sampling during molecular dynamics simulation. Journal of Molecular Graphics and Modelling, 2013, 46, 140-149.	2.4	11
60	Reconstruction of Three-Dimensional Conformations of Bacterial ClpB from High-Speed Atomic-Force-Microscopy Images. Frontiers in Molecular Biosciences, 2021, 8, 704274.	3.5	10
61	Conformational dynamics of human protein kinase CK2α and its effect on function and inhibition. Proteins: Structure, Function and Bioinformatics, 2018, 86, 344-353.	2.6	8
62	Hybrid Methods for Macromolecular Modeling by Molecular Mechanics Simulations with Experimental Data. Advances in Experimental Medicine and Biology, 2018, 1105, 199-217.	1.6	8
63	Gaussian mixture model for coarse-grained modeling from XFEL. Optics Express, 2018, 26, 26734.	3.4	8
64	Macromolecular Dynamics by Hybrid Electron Microscopy Normal Mode Analysis. Microscopy and Microanalysis, 2014, 20, 1218-1219.	0.4	7
65	Poisson image denoising by piecewise principal component analysis and its application in singleâ€particle Xâ€ray diffraction imaging. IET Image Processing, 2018, 12, 2264-2274.	2.5	5
66	Light-Control over Casein Kinase $1\hat{l}^{\prime}$ Activity with Photopharmacology: A Clear Case for Arylazopyrazole-Based Inhibitors. International Journal of Molecular Sciences, 2022, 23, 5326.	4.1	5
67	Searching for 3D structural models from a library of biological shapes using a few 2D experimental images. BMC Bioinformatics, 2018, 19, 320.	2.6	4
68	Computational investigation of the conformational dynamics in Tom20â€mitochondrial presequence tethered complexes. Proteins: Structure, Function and Bioinformatics, 2019, 87, 81-90.	2.6	4
69	Conformational ensemble of an intrinsically flexible loop in mitochondrial import protein Tim21 studied by modeling and molecular dynamics simulations. Biochimica Et Biophysica Acta - General Subjects, 2020, 1864, 129417.	2.4	4
70	Cryo-Cooling Effect on DHFR Crystal Studied by Replica-Exchange Molecular Dynamics Simulations. Biophysical Journal, 2019, 116, 395-405.	0.5	3
71	Crystal contact-free conformation of an intrinsically flexible loop in protein crystal: Tim21 as the case study. Biochimica Et Biophysica Acta - General Subjects, 2020, 1864, 129418.	2.4	3
72	Computational Protocol for Assessing the Optimal Pixel Size to Improve the Accuracy of Single-particle Cryo-electron Microscopy Maps. Journal of Chemical Information and Modeling, 2020, 60, 2570-2580.	5.4	3

#	Article	IF	CITATIONS
73	Parameter optimization for 3D-reconstruction from XFEL diffraction patterns based on Fourier slice matching. Biophysics and Physicobiology, 2019, 16, 367-376.	1.0	2
74	Protocol for Retrieving Three-Dimensional Biological Shapes for a Few XFEL Single-Particle Diffraction Patterns. Journal of Chemical Information and Modeling, 2021, 61, 4108-4119.	5.4	1
75	Elastic image registration to fully explore macromolecular dynamics by electron microscopy. , 2014, , .		0
76	Editorial overview: Macromolecular assemblies. Current Opinion in Structural Biology, 2017, 43, vii-ix.	5.7	0